Original Article

Improved Lateral Cephalometric Superimposition Using an Automated Image Fitting Technique

Brent E. Larson[a]; Matthew M. Sievers[b]; Ching-Chang Ko[c]

ABSTRACT

Objective: To test the feasibility of automated lateral cephalometric radiograph (LCR) superimposition using an image fitting algorithm.

Materials and Methods: Using radiopaque markers, we identified seven cephalometric landmarks on three dry skulls, took digital LCRs on each in several rotated positions, and used a custom software program (XRay3D) to automatically superimpose each rotated image on the initial image using an anterior cranial base reference. We measured superimposition error at each landmark and adjusted image brightness levels to simulate potential fitting error due to exposure variation.

Results: The greatest mean error for 24 image rotation trials of less than 10° was less than 0.5 mm. Rotations of 10° or more were not reliably superimposed. Errors of 0.2–1.6 mm occurred for ±10% brightness but increased exponentially with further brightness alteration.

Conclusion: Automated superimposition of LCRs, using this fitting technique, has great potential when rotation is less than 10° and brightness variation is less than 10%. (*Angle Orthod.* 2010; 80:474–479.)

KEY WORDS: Cephalometrics; Superimposition; Digital

INTRODUCTION

Cephalometric superimposition is an important tool for assessing facial growth and orthodontic treatment effects.[1] Routine clinical assessment of overall skeletal growth requires the ability to superimpose on the relatively unchanging structures of the anterior cranial base.

Baumrind et al[2] investigated errors in cephalometric superimposition and found clinically significant errors when employing landmark-based superimposition techniques, especially when assessing individual patients. For this reason, gold standard superimposition techniques have involved hand tracing of relevant structures on acetate film and then manual superimposition of the two tracings based on the best fit of the anterior cranial base structures. Elmagian[3] defined the spheno-cribriform superimposition as "superimposition on the plane of the sphenoid bone and the cribriform plate, registered at the intersection of the midpoint of the curvature of the great wings." This is the basis of current American Board of Orthodontics requirement to present overall superimposition tracings registered on "the best fit on the anterior cranial base bony structures (Planum Sphenoidum, Cribiform Plate, Greater Wings of the Sphenoid)."[4]

Recent publications have shown that good superimpositions can be accomplished with current digital radiographs and available software, but these methods simply duplicate manual methods in the digital realm.[5,6] The operator must digitally trace relevant structures and still make a subjective best fit decision on how the two tracings should be related.

The purpose of this pilot project was to test the feasibility of using automated image fitting techniques to superimpose lateral cephalometric images on the anterior cranial base without the need to trace structures and to eliminate the operator bias in determining a best fit match.

[a] Associate Professor, Division of Orthodontics, Department of Developmental and Surgical Sciences, School of Dentistry, University of Minnesota, Minneapolis, MN.

[b] Resident, Division of Orthodontics, Department of Developmental and Surgical Sciences, School of Dentistry, University of Minnesota, Minneapolis, MN.

[c] Associate Professor, Department of Orthodontics, School of Dentistry, University of North Carolina, Chapel Hill, NC.

Corresponding author: Dr Brent E. Larson, Division of Orthodontics, Department of Developmental and Surgical Sciences, University of Minnesota, 6-320 Moos Tower, 515 Delaware St SE, Minneapolis, MN 55455
(e-mail: larso121@umn.edu)

Accepted: August 2009. Submitted: April 2009.

 DOI: 10.2319/042509-229.1

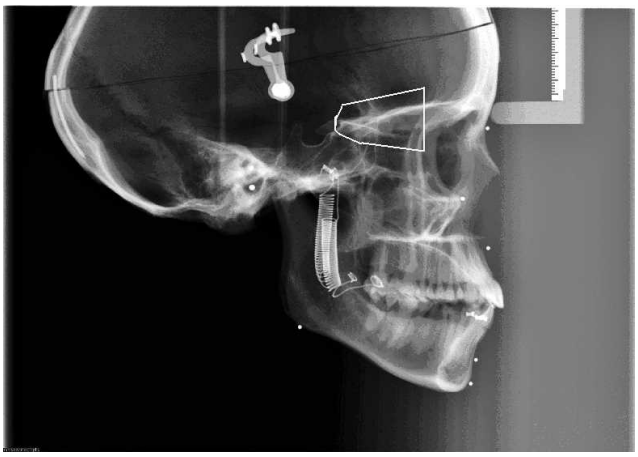

Figure 1. Image of lateral cephalometric radiograph (LCR) with radiopaque markers at cephalometric landmarks and an example of the superimposition region used in this study (white outline).

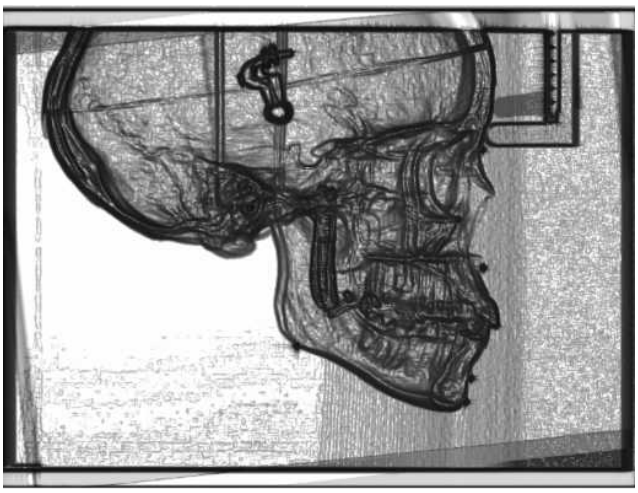

Figure 2. Screenshot showing a completed superimposition of two images. Note the angled shadows along the lower border, which indicate how much the second image was rotated and translated to match the first.

MATERIALS AND METHODS

Seven cephalometric landmarks (nasion, orbitale, A-point, B-point, pogonion, gonion, porion) were identified on three dry skulls (designated as A, B, and C) using spherical radiopaque markers. Digital lateral cephalometric radiographs (LCR) were taken on each skull in 13 different positions rotating around the ear rods of the cephalostat. These positions were an initial unrotated orientation with Frankfurt Horizontal parallel to the floor and then from 2° to 15° of rotation in both the clockwise and counterclockwise directions.

Rotation Trials

Following image acquisition, each rotated image was superimposed on the initial nonrotated image using the Xray3D program© developed by Dental Research Center for Biomaterials and Biomechanics at the University of Minnesota. This software, originally developed for assessing bone loss around implants,[7] uses a mathematical algorithm to match a selected area on one radiographic image to the most similar area on a second image. Initial trials indicated that successful image matching using this software was achieved using image matrices of 800 × 600 pixels and a sigma value of 20.

The superimposition process required defining the selected region the Xray3D program would use for image matching and the resulting superimposition. This allowed the software to superimpose the images using the entire topology of the selected region and to match it as accurately as possible to the other radiograph. The region used in this study included the sphenoid plane, cribriform plate, and the greater wings of the sphenoid bone as described originally by Elmagian.[3] Figure 1 shows an example of this region.

The Xray3D software is capable of image matching using all six degrees of freedom, but for this application, rotation was allowed only around the z-axis and translation only in the x and y directions. These restrictions ensured that the LCR would be translated and/or rotated in only a two-dimensional plane (analogous to placing one radiograph or tracing on top of the other and translating and rotating them to the best fit possible). The automated superimposition process was completed in two steps: first, a rough fit (Xray3D normal fit) using 30% of the points, and then refining that position with a complete fit (Xray3D total fit) that used 100% of the points. After the fitting process was complete, the root mean square (RMS) values were recorded for each of the two steps (normal and total fit). Figure 2 shows a screen image of the completed superimposition of two LCR images.

The accuracy of the superimposition was assessed by measuring the difference in landmark position from one image to its superimposed pair. Because no growth occurred in the skulls between images, a perfect cranial base fit would result in a zero difference in landmark locations after automated superimposition. The measurements were made by importing both the initial unrotated image and the superimposed image into Adobe Photoshop (Adobe Systems, Inc, San Jose, CA). The pixel location of each radiographic landmark was determined on the reference image and compared with the pixel location of each landmark on the superimposed image. The superimposition error was quantified by calculating the difference in pixel location, and this pixel difference was then converted into millimeters of error based on the image resolution. The average superimposition error was calculated using all landmarks, and this average was recorded for each rotational trial.

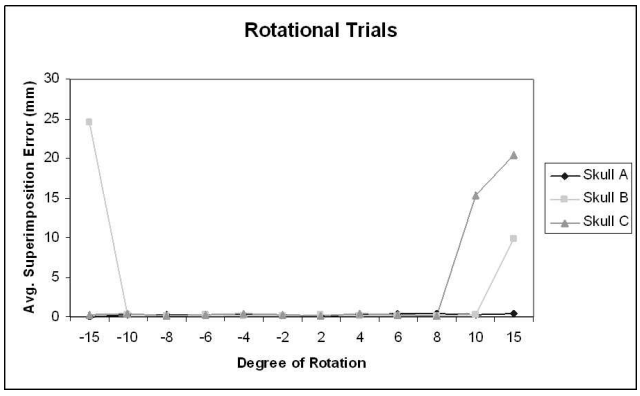

Figure 3. Plot of rotational trials data by skull showing the all-or-nothing effect of fitting success.

Brightness Trials

The effect of exposure variation on superimposition using the Xray3D algorithm was simulated using the same three skulls by manipulating the brightness level of the radiographs using Adobe Photoshop tools. The neutral rotation and the 6° clockwise rotated images were used for these trials. The 6° clockwise rotated image was modified to −60%, −40%, −30%, −20%, −10%, +10%, +20%, +30%, +40%, or +60% brightness. Each resulting image was then superimposed on the neutral brightness reference image for the corresponding skull. The superimposition procedure for these trials was identical to the procedure described for the rotation trials. The unaltered 6° clockwise image was also superimposed against the reference image. The average superimposition error for the landmarks was calculated as was done for the rotation trials.

Reproducibility

All rotation and brightness trials were repeated for skull A to determine whether the automated superimpositions were reproducible. These trials were done at a different session than the original trials and included redefining the fit area for each superimposition.

For the purpose of this feasibility study, landmark errors of ≤0.5 mm were defined as sufficiently accurate for further development of the automated process.

RESULTS

Because the radiopaque marker locating porion was not identifiable because of the dense bone in the region, this landmark was not included in the analysis, and all trial averages included only six cephalometric landmarks.

Rotation Trials

Skulls A, B, and C were accurately superimposed for all trials rotated 8° or less, as shown in Figure 3. The greatest mean error for the 24 rotation trials of less than 10° was below 0.5 mm (range, 0.1–0.4). All average landmark errors and RMS values for the rotation trials are shown in Table 1. The skull C image rotated 15° counterclockwise was the only image with this degree of rotation that superimposed accurately, demonstrating that superimposition is possible for the algorithm at higher levels of rotation under certain conditions (average superimposition error of 0.27 mm). Any rotation trial with an RMS value in excess of 1000 demonstrated erroneous superimposition (the highest RMS value for accurate superimposition was 608.8). An all-or-nothing response of superimposition accuracy was noted with this method: all trials were either accurately superimposed or far from accurate, with no trials demonstrating a middle ground.

Table 2 gives the average superimposition error for each cephalometric landmark for all rotation trials of 8° or less rotation in either direction. Results show that orbitale and gonion were the most accurate, with mean superimposition errors of 0.20 mm for the three skulls

Table 1. Rotation Trials Data for All Three Skulls

	Skull A		Skull B		Skull C		All
Rotation, °	Average Error, mm	RMS	Average Error, mm	RMS	Average Error, mm	RMS	Average Error, mm
−15	NA	NA	24.45	2055.8	0.27	539.4	12.36
−10	0.33	566.8	0.35	176.3	0.41	430.7	0.36
−8	0.31	324	0.12	135.7	0.21	338.9	0.21
−6	0.35	161.3	0.33	198.1	0.25	213.6	0.31
−4	0.35	96	0.1	138.8	0.41	366.1	0.29
−2	0.28	160.9	0.17	90.9	0.31	363.6	0.25
2	0.21	75	0.31	83.5	0.21	395	0.24
4	0.31	338.7	0.17	106.6	0.42	449.7	0.3
6	0.43	491.7	0.1	150.5	0.24	504.5	0.26
8	0.38	484.4	0.21	167.1	0.17	608.8	0.25
10	0.35	390.1	0.32	284.4	15.29	3755.8	5.32
15	0.39	538	9.84	1260.4	20.41	3588.9	10.21

Table 2. Combined Superimposition Error for All Rotational Trials ≤8° by Landmark

Landmark	Skull A, mm	Skull B, mm	Skull B, mm	3 Skull Average, mm
Nasion	0.36	0.22	0.11	0.23
Orbitale	0.18	0.18	0.25	0.2
A-Point	0.37	0.22	0.26	0.28
B-Point	0.34	0.26	0.35	0.32
Pogonion	0.34	0.14	0.54	0.34
Gonion	0.39	0.11	0.11	0.2

combined. The range of mean superimposition error was narrow, ranging from 0.20 to 0.34 mm.

Brightness Trials

Brightness alterations of skulls A, B, and C had the greatest superimposition accuracy when change was limited to ±10%. Figure 4 indicates that the superimposition error does not show the all-or-nothing response of the rotation trials but instead demonstrates progressively increasing error with increasing brightness alteration. The mean superimposition error for trials of 10% alteration or less ranged from 0.2 to 1.6 mm, as shown in Table 3.

Reproducibility

In a complete repeat of the entire series of skull A rotational trials, the resulting data are nearly identical, as shown in figures 5 and 6.

DISCUSSION

This pilot study indicates that with the software in its current form, it is possible to superimpose LCRs accurately without the use of landmarks, when images are rotated less than 10° and with brightness minimally altered (between ±10%).

Data from the rotational trials and brightness trials indicate at least one major difference: the all-or-nothing accuracy of the superimpositions in the rotational trials. This all-or-nothing result is apparent in the rotational trials for all three skulls, where superimpositions are accurate until suddenly with increasing rotation they become exceptionally inaccurate. The Xray3D program apparently finds a local minimum registration that it deems the best fit, instead of continuing to rotate and translate the image into the actual best fit superimposition. Modification of the Xray3D fitting algorithm may minimize or eliminate this problem. The sudden rotation error effect contrasts with the gradually increasing error that results from incremental changes in brightness differences among images. The rotational error should not pose a clinical problem since patient positioning in the cephalometric machine makes rotations of 10° or more unlikely. Error

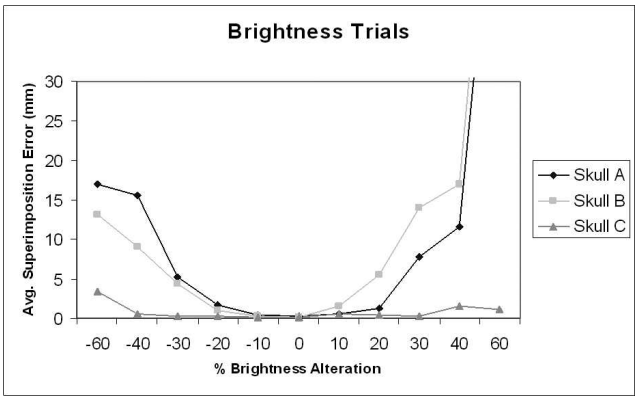

Figure 4. Plot of brightness trials data by skull showing progressive error with increasing brightness variation.

could also be eliminated by using a landmark-based preliminary fit, followed by the automated superimposition for the final objective superimposition. Errors due to variation in image brightness may be more difficult to detect, so applying this algorithm to actual patients will require awareness of the importance of proper image exposure or possibly normalization of the image density prior to superimposition.

The significance of the RMS value in assessing the accuracy of the superimposition must also be considered when evaluating these results. The RMS values for the skull A rotation trials had little or no correlation with the accuracy of fit, while they increased dramatically for skulls B and C when the superimposition failed completely. The significance of the RMS value appears to be in its variation among trials in the same set. An arbitrary threshold of RMS values greater than 1000 could indicate a need to evaluate the accuracy of the superimposition and should be better defined though clinical trials.

An important step in the Xray3D superimposition process involved defining the superimposition area, a region both repeatedly identifiable and stable over time for use in longitudinal studies. The area used in this study was the anterior cranial base region described by Elmagian[3] in 1959 in a detailed longitudinal study of the skeletal morphology of the anterior cranial base, in an effort to determine its most stable element(s). That research was stimulated by Brodie,[8] whose 1941 study determined that after 5 years of age, little change in the anterior cranial base occurs. This study used the highly stable region defined in the study by Elmagian,[3] demonstrated by the plane of the sphenoid bone and the cribriform plate, registered at the intersection of the midpoint of the curvature of the great wings with the sphenoid plane-cribriform plate contour. A benefit to using the entire topology of a region is that small errors in region boundary identification do not lead to large errors in superimposition, as is the case with current

Table 3. Brightness Variation Trials Data for All Three Skulls

	Skull A		Skull B		Skull C		All
Brightness, %	Average Error, mm	RMS	Average Error, mm	RMS	Average Error, mm	RMS	Average Error, mm
−60	17	2698.9	13.18	3018.7	3.45	3757.5	11.21
−40	15.63	2453.7	9.02	1809	0.55	2578.5	8.4
−30	5.18	1969.9	4.43	1360.3	0.28	1880.9	3.3
−20	1.75	1307	1.02	735.1	0.3	1188.2	1.02
−10	0.46	641.2	0.33	171.4	0.19	575.3	0.33
0	0.33	466.2	0.15	152.6	0.17	498.2	0.22
10	0.55	356.9	1.55	750.9	0.53	444.3	0.88
20	1.33	961.3	5.52	1385.6	0.36	1010.2	2.4
30	7.79	1745.7	13.94	1703.6	0.33	1662.8	7.35
40	11.57	2093.6	17	2076.8	1.61	2322.2	10.06
60	64.13	5996.6	72.1	4365.3	1.12	3613.9	45.78

landmark-based superimposition. Our repeated skull A superimposition studies produced consistent results, even though the defined superimposition region had to be manually selected for each trial and thus the boundaries were undoubtedly slightly different.

Using three different skulls allowed for testing the effectiveness of superimposition with varying anterior cranial base morphology. In rotational trials, differences between the skulls did not manifest as differences in superimposition accuracy. The results of the skull C brightness trials demonstrated tolerance to brightness variation compared with the other two skulls, probably because on skull C, the springs that hold the mandible to the skull are attached more superiorly and consequently were included in the superimposition region. The result was a very radiopaque area of high contrast that the Xray3D program could clearly identify in all of the altered brightness images for that skull and use to superimpose more accurately. The springs on the other skulls were not located in the superimposition area.

A limitation of this study is that because the images were obtained from dry skulls rather than humans, they had no growth changes that may make superimposition more difficult for the Xray3D program. The skull images also do not have soft tissue, which results in better contrast in the area of superimposition. Clinical trials are a logical next step in testing this methodology. A sufficient clinical sample could allow statistical testing of the hypothesis that automated superimposition using image fitting algorithms is comparable to conventional superimpositions done by experienced experts.

Development of this automated superimposition technique has several possible advantages. Incorporation into routine clinical imaging programs could provide immediate and accurate feedback to clinicians relative to growth and treatment effects. In addition, when used for research purposes, it could provide an objective and unbiased method for superimposition of lateral cephalometric films to eliminate operator error or bias.

CONCLUSION

- This feasibility study demonstrates a novel method of superimposing cephalometric radiographs using the entire topology of the anterior cranial base.
- Accurate superimposition is achievable on a dry skull using image fitting algorithms for which the rotation of the image is within 10° and the radiograph brightness is within ±10%.

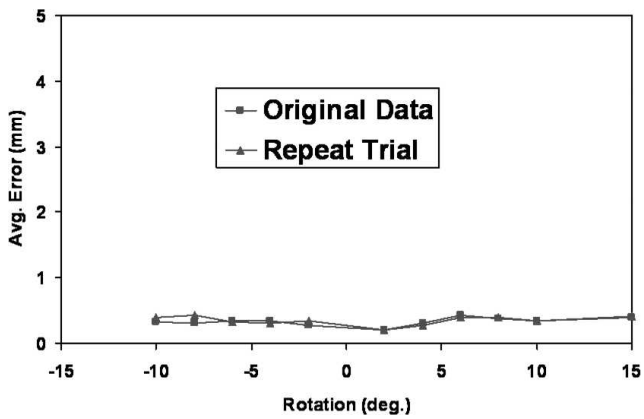

Figure 5. Plot of skull A rotational data: original and repeated trial.

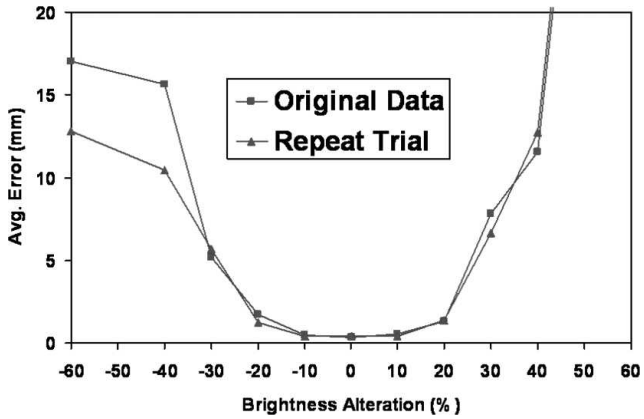

Figure 6. Plot of skull A brightness data: original and repeated trial.

- Clinical testing is warranted to determine whether this automated superimposition could be developed as a useful clinical assessment and research tool.

REFERENCES

1. Proffit WR. *Contemporary Orthodontics*. 4th Ed. St Louis, MO: Mosby; 2007.
2. Baumrind S, Miller D, Molthen R. The reliability of head film measurements: tracing superimposition. *Am J Orthod*. 1976; 70:617–644.
3. Elmagian K. *A Serial Study of Facial Growth as Related to Cranial Base Morphology* [thesis]. Seattle, WA: University of Washington; 1959.
4. American Board of Orthodontics Web site. Presentation of case reports, composite tracings, craniofacial composite. Available at: http://www.americanboardortho.com/professionals/clinicalexam/casereportpresentation/preparation/tracings. Accessed April 24, 2009.
5. Roden-Johnson D, English J, Gallerano R. Comparison of hand-traced and computerized cephalograms: landmark identification, measurement, and superimposition accuracy. *Am J Orthod Dentofacial Orthop*. 2008;133:556–564.
6. Huja S, Grubaugh EL, Rummel AM, Fields HW, Beck FM. Comparison of hand-traced and computer-based cephalometric superimpositions. *Angle Orthod*. 2009;79:428–435.
7. Ko CC, Douglas WH, DeLong R, Rohrer MD, Swift JQ, Hodges JS, An K-N, Ritman EL. Effects of implant healing time on crestal bone loss of a controlled-load dental implant. *J Dent Res*. 2003;82:585–591.
8. Brodie AG. On the growth pattern of the human head from the third month to the eighth year of life. *Am J Anat*. 1941;68: 209–262.